

Charge imbalance and magnetic properties at the $\text{Fe}_3\text{O}_4/\text{BaTiO}_3$ interface

Min Sik Park, Jung-Hwan Song, and Arthur J. Freeman

Department of Physics and Astronomy, Northwestern University, Evanston, Illinois 60208, USA

(Received 28 April 2008; revised manuscript received 9 December 2008; published 20 January 2009)

The electronic structure and physical properties at the interface in the superlattice $\text{Fe}_3\text{O}_4/\text{BaTiO}_3$ were investigated by using the first-principles all-electron full-potential linearized augmented plane-wave method. The loss of half metallicity of bulk Fe_3O_4 in the multiferroic superlattice $\text{Fe}_3\text{O}_4/\text{BaTiO}_3$ is related to the charge imbalance effect at the interface. The effect of strain strongly influences the Fe magnetic moments and the spin-polarized carriers at the interface. Oxygen vacancies are shown to recover the almost half-metallic ground state in the superlattice. The effects of the charge imbalance, the strain, and the oxygen vacancies at the interface in the superlattice $\text{Fe}_3\text{O}_4/\text{BaTiO}_3$ can be applied to designing better multifunctional oxide-based systems.

DOI: 10.1103/PhysRevB.79.024420

PACS number(s): 75.70.Cn, 75.80.+q, 73.20.-r

I. INTRODUCTION

The emergence of multiferroic materials in applications for multifunctional devices makes it very important to understand the interplay between ferromagnetic (or ferrimagnetic) and ferroelectric properties, where it is required that the ferromagnetic property is controlled by an applied electric field and vice versa. There are some bulk-type (single phase) multiferroic materials, such as BiMnO_3 , CdCr_2S_4 , and BiFeO_3 , etc.; however, they have low Curie temperature (below 135 K) or low reproducibility.¹ On the contrary, by choosing the appropriate bulk materials, two phase systems made by contact between two different single phase materials can be robust at room temperature.¹ Among two phase systems, superlattices and films are especially good candidates for studying the relations between ferromagnetic and ferroelectric properties rather than single phase materials since they interact with each other only through the interface. Thus, it is important to study the interfaces in the multiferroic devices in the form of superlattices and films, in which the interface plays a decisive role in determining their functionality since its physical properties are different from those of the bulk materials.

The physical properties of these interfaces are, however, not well known in multiferroic thin films and superlattices. To understand them, the $\text{Fe}_3\text{O}_4/\text{BaTiO}_3$ superlattice has been studied in this paper. Now, spinel magnetite Fe_3O_4 has a ferrimagnetic ground state (total magnetic moment of $4.33\mu_B$ and $T_C \sim 860$ K)^{2,3} and a high spin polarization, and perovskite BaTiO_3 has a ferroelectric tetragonal structure at room temperature (saturation ferroelectric polarization 0.26 C/m² and $T_C \sim 393$ K).⁴ Given these strong ferroic properties, superlattices of these materials are good candidates for possible multiferroic applications. However, the effect of the interface on the electronic properties of the superlattice, which will eventually affect ferromagnetic and ferroelectric properties, should be clarified first.

In this paper, for the study of the $\text{Fe}_3\text{O}_4/\text{BaTiO}_3$ superlattice, the highly precise all-electron full-potential linearized augmented plane-wave (FLAPW) method^{5,6} is used, and a number of important issues are discussed. First, theoretically whereas bulk Fe_3O_4 is half metallic, the half metallicity in our calculations is destroyed at the interface in the

$\text{Fe}_3\text{O}_4/\text{BaTiO}_3$ superlattice. Even though this loss of half metallicity by interface states was reported in previous works for several Heusler/semiconductor interfaces, such as $\text{Co}_2\text{MnGe}/\text{GaAs}$ (Ref. 7) and $\text{Co}_2\text{CrAl}/\text{InP}$ (Ref. 8), the reason behind the loss is still not clear. As one possible mechanism, the effect of charge imbalance is proposed in Sec. III A. Second, experimentally, it has been reported that strain affects the magnetic properties of Fe_3O_4 with the different substrates and in superlattices.⁹⁻¹⁴ However, to our knowledge, there are theoretical studies only for the bulk strain effect.^{15,16} In Sec. III B, we discuss the strain effect at the interface due to charge imbalance which cannot occur in the bulk. Moreover, recently it was reported that the strongly bias-dependent magnetoresistance at the $\text{Fe}_3\text{O}_4/\text{BaTiO}_3$ barrier is measured in a multiferroic $\text{Fe}_3\text{O}_4/\text{BaTiO}_3$ bilayer.² In this experiment, the sign of the magnetoresistance is switched from negative at low bias to positive at high bias, which shows well the interaction between magnetic and ferroelectric properties in the $\text{Fe}_3\text{O}_4/\text{BaTiO}_3$ bilayer. Here, we discuss the change in the spin polarization of carriers¹⁷ through the strain at the interface, which is possibly controlled by an external electric field. Finally, in the oxides systems, oxygen vacancies can be considered in many cases to play an important role. In Sec. III C, we show that indeed oxygen vacancies can recover the half metallicity destroyed by charge imbalance in the oxide multiferroic superlattice and thus increase the spin polarization of the carriers. We show that the results from these oxygen-vacancy effects can be explained by a shift of E_F to a higher energy level, which accordingly causes the change in the magnetic moments of Fe ions in the superlattice.

II. DETAILS OF THE CALCULATIONS

For a study of the $\text{Fe}_3\text{O}_4/\text{BaTiO}_3$ interface, we investigate the electric and magnetic properties of their superlattices by using the FLAPW method with the local exchange-correlation scheme formulated by Hedin and Lundqvist.¹⁸ We use a half unit cell of spinel Fe_3O_4 ,¹⁹ and one and a half unit cells of perovskite BaTiO_3 (Ref. 20) for constructing the supercell in the experimentally reported [001] direction¹³ [Fig. 1(a)]. The interface in the superlattice is composed of

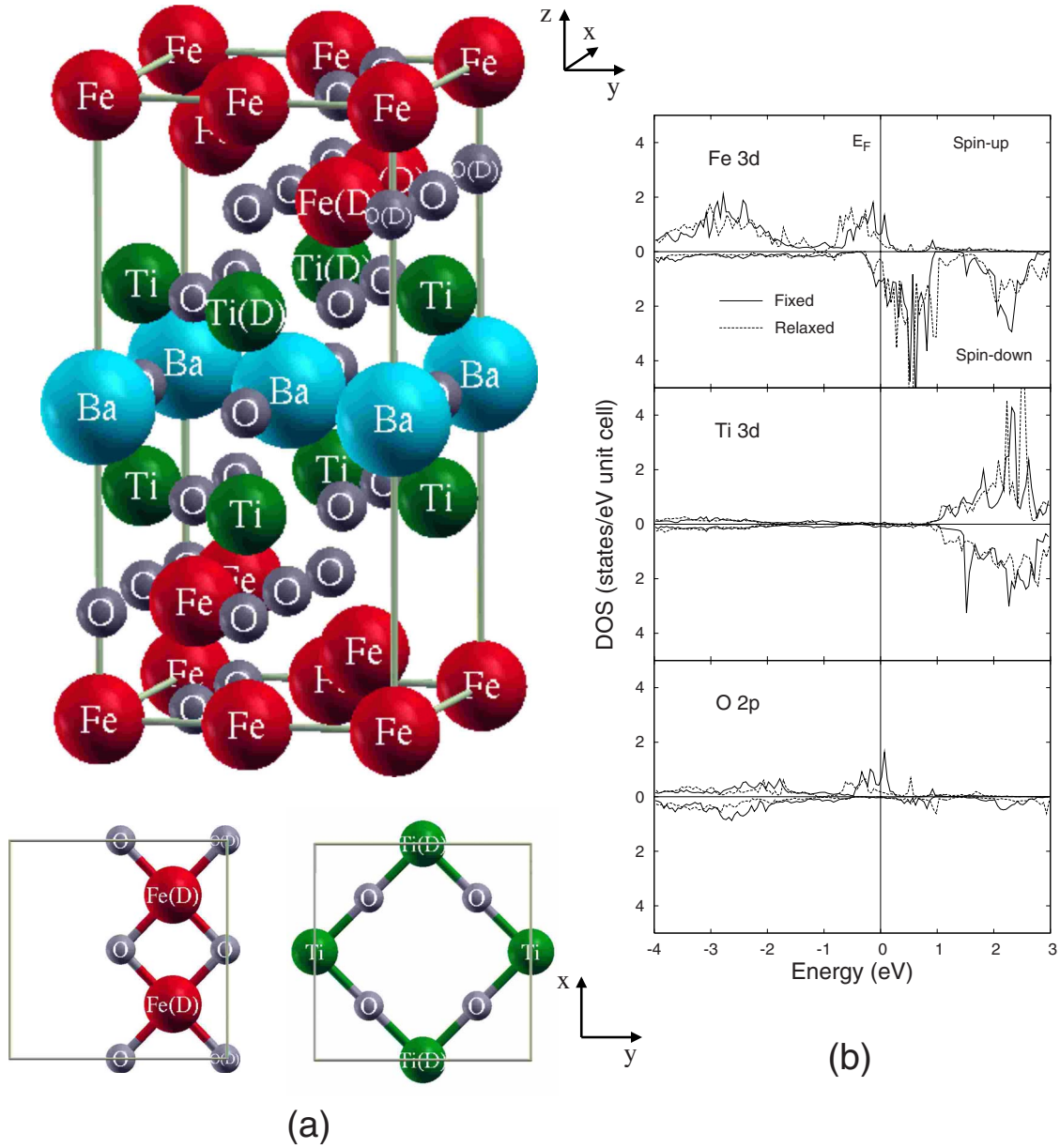


FIG. 1. (Color online) (a) (upper) Crystal structure of the superlattice $\text{Fe}_3\text{O}_4/\text{BaTiO}_3$, (lower left) interfacial Fe_2O_4 layer, (lower right) interfacial TiO_2 layer, and (b) projected DOS of octahedral Fe $3d$, Ti $3d$, and O $2p$ states at the interface, where the O $2p$ state is located in the interfacial Fe_2O_4 layer. These atoms are marked on (a) by Fe(D), Ti(D), and O(D), respectively. (solid line: fixed structure; dotted line: relaxed structure).

$(\text{Fe}_2\text{O}_4)^{3-}$ and $(\text{TiO}_2)^0$ layers from Fe_3O_4 and BaTiO_3 , respectively,²¹ to match the Fe-O bonds more efficiently. Three kinds of in-plane lattice constants are considered from the spinel Fe_3O_4 (8.398 Å), perovskite BaTiO_3 (7.988 Å = 2×3.994 Å), and average lattice constants are taken for the study of the strain effect. If not otherwise specified, the superlattice with spinel Fe_3O_4 lattice constant is mainly considered here, which corresponds to a direct structure.² Next, atomic structure relaxation was also performed in all directions for all superlattices. The magnetic moments of ions are considered only inside muffin-tin spheres of 2.0, 2.1, 1.5 a.u. for Fe, Ti, O ions, respectively, in the fixed structure, and for the relaxed structure, muffin-tin spheres of 1.3 and 1.4 a.u. for the oxygen ions are employed. Energy cutoffs of 3.873

Ry and 250 Ry are employed for the plane-wave basis and the potential representation, respectively. An expansion in terms of spherical harmonics with angular momenta up to $l = 8$ is used to describe the wave functions inside the muffin-tin spheres. For the k mesh and the k -point integrations, a $15 \times 15 \times 7$ and the improved tetrahedron scheme^{22,23} are adopted, respectively.

III. RESULTS AND DISCUSSIONS

A. Loss of half-metallic property

Whereas the ground states of bulk cubic Fe_3O_4 and tetragonal BaTiO_3 are a half metal²⁴ and an insulator,²⁵ respec-

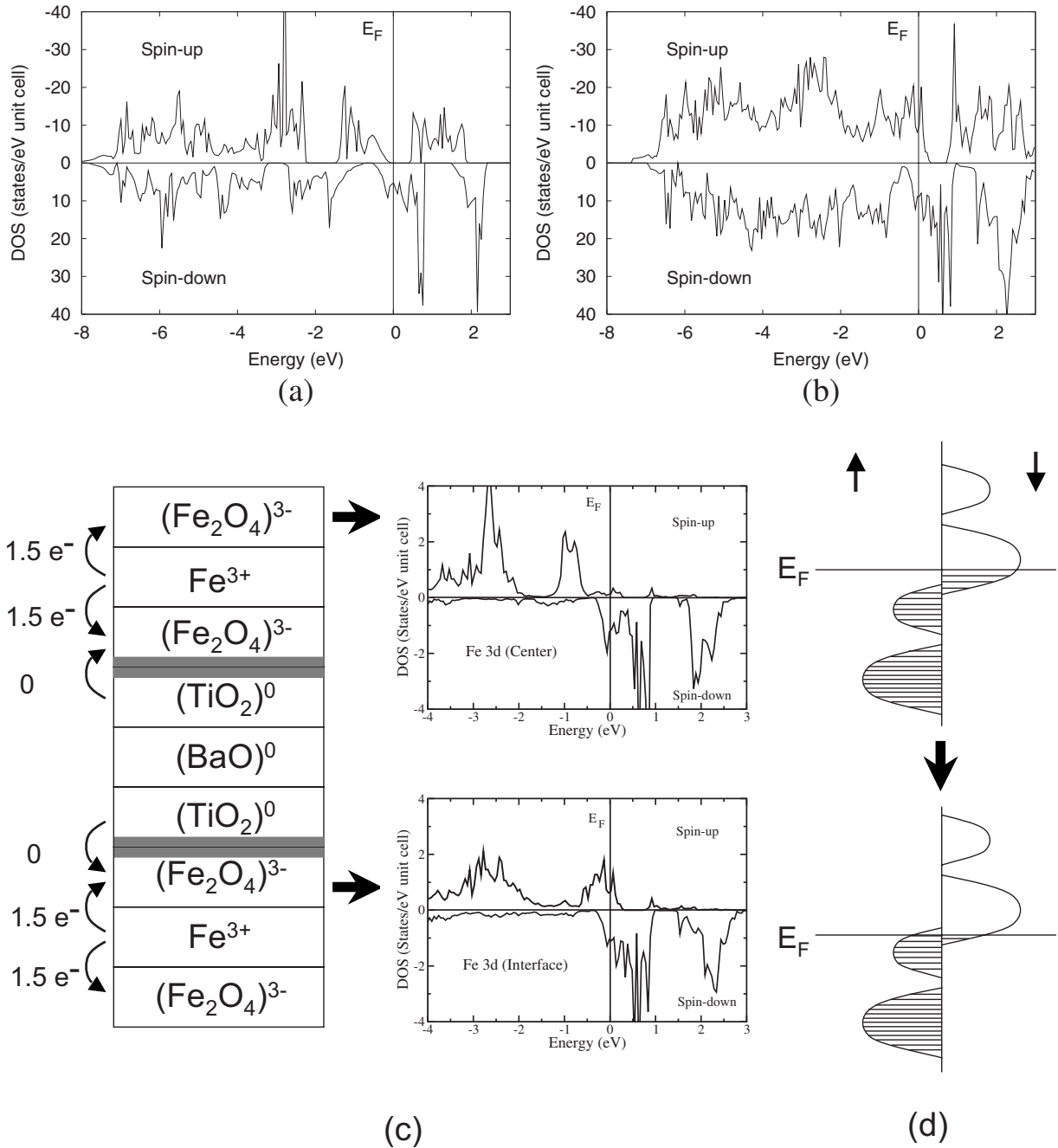


FIG. 2. Total DOS for (a) the bulk Fe₃O₄ and (b) the Fe₃O₄/BaTiO₃ superlattice with the fixed structure; (c) schematic diagram of the charge imbalance model and projected DOS of octahedral Fe 3d at the central and interfacial Fe₂O₄ layers and (d) schematic diagram of the change in 3d DOS for the octahedral Fe ion from the bulk Fe₃O₄ to the Fe₃O₄/BaTiO₃ superlattice by the charge imbalance.

tively, a simple metallic ground state is obtained for the Fe₃O₄/BaTiO₃ superlattice in both the fixed and relaxed structures [Fig. 1(b)]. From an analysis of the projected density of states (DOS), we find that the 3d states of Ti ions in the superlattices do not contribute to the DOS near the Fermi energy (E_F) [Fig. 1(b)]—a result that is different from previous Fe/BaTiO₃ calculations, which show hybridization between the Ti 3d and Fe 3d orbitals.²⁶ In our results, such a hybridization is absent since the Ti 3d orbitals can interact with Fe 3d only through the interfacial oxygen 2p orbitals. Moreover, considering our result of unoccupied Ti 3d orbitals, we do not expect any serious problems (e.g., partially

occupied Ti 3d orbitals) in our calculated results, which may be caused by the possible underestimated band gaps in the local-density approximation (LDA) scheme. Therefore, a metallic ground state different from the half-metallic ground state of bulk Fe₃O₄ [compare Figs. 2(a) and 2(b)] originates from a change in the Fe 3d states and the oxygen 2p states near E_F. In Figs. 2(a) and 2(b), the total DOS of the Fe₃O₄/BaTiO₃ superlattice is compared to that of the bulk Fe₃O₄ instead of the bulklike part of the superlattice for clarity since the bulklike Fe atoms in the central layer in the Fe₃O₄ part of the superlattice do not show the clear nominally half-metallic property [as seen on the projected DOS

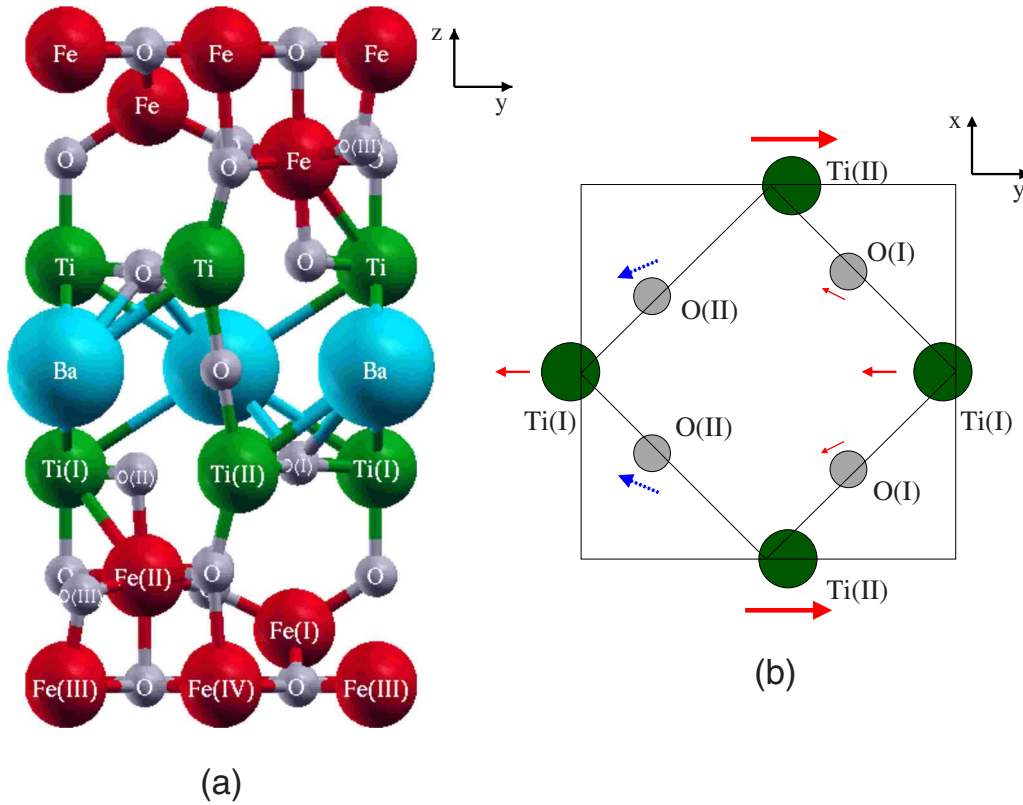


FIG. 3. (Color online) (a) Crystal structure for the relaxed atomic position of superlattice $\text{Fe}_3\text{O}_4/\text{BaTiO}_3$ and (b) displacement of Ti and O ions in the TiO_2 plane, where the length of arrows is proportional to the displacement of ions, and the solid-line and the dotted-line arrows mean the slight displacement toward up and down, respectively.

for Fe $3d$ in the central layer in Fig. 2(c)] by its short period supercell geometry. The destruction of half metallicity in the $\text{Fe}_3\text{O}_4/\text{BaTiO}_3$ superlattice is caused by the charge imbalance at the interface, in which the interfacial $(\text{Fe}_2\text{O}_4)^{3-}$ layer lacks 1.5 electrons for the charge neutralization, since the BaTiO_3 has the insulating surface and thus the $(\text{TiO}_2)^0$ layer in the BaTiO_3 does not contribute electrons to the $(\text{Fe}_2\text{O}_4)^{3-}$ layer [Fig. 2(c)]. Therefore the valence of Fe ions near the interface is changed, which shifts the Fermi energy to the lower energy level, and destroys the half metallicity of bulk Fe_3O_4 [Fig. 2(d)]. Indeed, the projected DOSs of Fe $3d$ from the interfacial and central layers show the evident depth profile of the metallic and half-metallic properties, respectively [Fig. 2(c)]. In addition, from our projected DOS results for the larger superlattice with one unit cell of Fe_3O_4 ,¹⁹ the more evident change is seen from the interfacial metallicity to the central half metallicity. Hence, the interface properties in our study are not affected by the superlattice thickness, specifically, beyond the half-unit-cell thickness of the Fe_3O_4 part. Moreover, charges inside the muffin-tin radius of Fe ions in the superlattice decrease by as much as $0.13\text{--}0.16e^-$ compared to bulk Fe_3O_4 ; however, the case of oxygen ions shows a negligible decrease of $0.02\text{--}0.05e^-$. This lack of half metallicity at the interface may cause several problems such as lower spin-polarization and possibly stronger screening of the dipolar field in ferroelectric materials.^{27,28}

B. Strain effect on magnetic properties

The Fe magnetic moments in the superlattice with the fixed structure are similar to those in bulk Fe_3O_4 , which are

-3.3 and $3.43\mu_B$ for the tetrahedral and octahedral Fe ions, respectively. From Fig. 3(a), the four types of Fe ions are marked as Fe(I) in the tetrahedral site and Fe(II), Fe(III), and Fe(IV) in the octahedral sites, and have magnetic moments of -3.3 , 3.36 , 3.39 , $3.53\mu_B$, respectively, which shows a ferrimagnetic ground state as in bulk Fe_3O_4 . The notable thing is the large induced magnetic moment of oxygen at the interface; these oxygen atoms are located in the plane with the Fe(II) ion and have moments of 0.21 and $0.25\mu_B$, which are three times larger than in the bulk Fe_3O_4 system. These induced magnetic moments can be explained by the charge imbalance at the interface, in which the hybridized spin-polarized partially empty $2p$ states of interfacial oxygen atoms are generated by the shifted E_F , which causes metallicity in Fe ions [see projected DOS of O $2p$ in Fig. 1(b)]. Interestingly, the geometry optimization shows a noticeable decrease in the Fe(III) magnetic moment in all superlattices with different lattice constants. That is, the Fe(III) magnetic moment is reduced by 0.64 , 1.37 , and $1.1\mu_B$ for the superlattices employing the bulk Fe_3O_4 , the bulk BaTiO_3 , and their average lattice constants, respectively [Fig. 4(c)]. As seen from Fig. 3(a), the upper and lower oxygen atoms, O(III), of the Fe(III) ion are tilted, that is, shifted from the apical axis parallel to the d_{z^2} state of the Fe(III) ion. Therefore, the spin-up d_{z^2} state of Fe(III) near E_F becomes a lower energy level than the $d_{x^2-y^2}$ state under the crystal-field scheme, which results in the unoccupied split spin-up state. Moreover, the magnetic moment of Fe(III) is reduced by the increase in the number of electrons in the spin-down (minor-

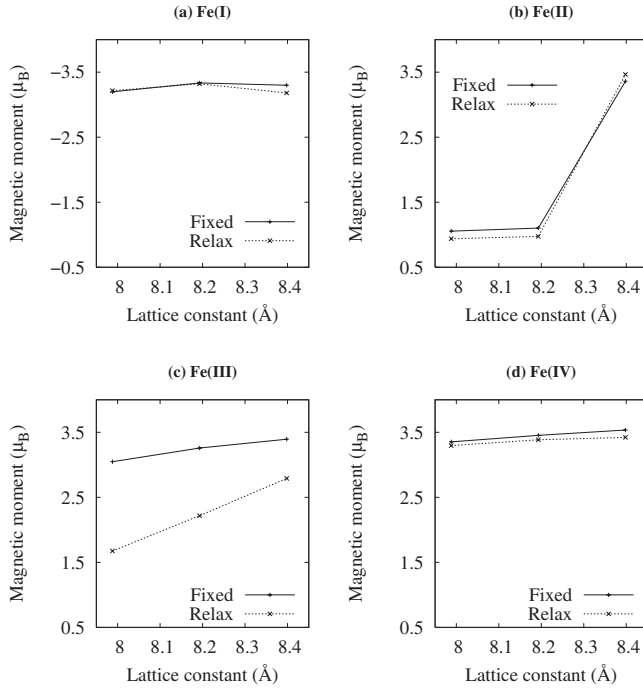


FIG. 4. The change in magnetic moments of (a) Fe(I), (b) Fe(II), (c) Fe(III), and (d) Fe(IV) ions marked in Fig. 3(a) by the atomic position relaxation and the strain. The lattice constants, 7.988, 8.193, and 8.398 Å, correspond to the lattice constants of BaTiO₃, average, and Fe₃O₄. For all superlattices, the constraint of fixed volume is applied.

ity) t_{2g} states near E_F , which comes from the reduced occupation of the spin-up (majority) $d_{x^2-y^2}$ state due to its shift to higher energy.

With the atomic position relaxation of the whole superlattice, we have obtained large displacements of the Ti and O ions. In the TiO₂ plane, the distance between Ti and O ions are changed in the [110] direction of the bulk BaTiO₃ by as much as -0.013, -0.133, -0.231, and 0.417 Å for the Ti(I)-O(I), Ti(I)-O(II), Ti(II)-O(I), and Ti(II)-O(II) pairs, respectively [Fig. 3(b)]. This corresponds to a monoclinic r phase^{29,30} being stable at positive misfit strains of the lattice constant of bulk Fe₃O₄. By these large atomic displacements in the TiO₂ and Fe₂O₄ layers, the instability caused by the high DOS at E_F of the fixed structure superlattice is reduced much, which stabilizes the Fe₃O₄/BaTiO₃ superlattice as much as 0.15 eV/unit cell compared to the fixed structure. In addition, the in- and out-of-plane symmetries are broken at the heterointerface of the Fe₂O₄ and TiO₂ layers, which may affect the atomic displacement. Further, to see the relation between the displacements of BaTiO₃ and Fe₃O₄ in the superlattice, only the relaxation of Fe₃O₄ layers was performed, and this shows similar relaxed atomic positions of the Fe and O ions as that of the relaxation of the whole superlattice. Thus, it is envisioned that the displacement of the Fe₃O₄ is independent of the displacement of the BaTiO₃, and originates mainly from the discontinuity of the crystal structures inducing atomic bonding mismatches at the interface. The change in magnetic moment by relaxation is, however, slightly different between the above two cases. In the case of the relaxation of the Fe₃O₄ only, the Fe(II) has

smaller magnetic moment (by $0.2\mu_B$) than those in the case of the whole structure relaxation, and the Fe(III) also has a smaller magnetic moment (by $0.15\mu_B$). These results show that the displacements of Ti ions by relaxation also contribute to the physical properties of the interfaces in the superlattices.

The strain effect also shows interesting results for the Fe magnetic moments. In the smaller lattice constants (BaTiO₃ and average), the crystal symmetry of the magnetite in the superlattice is not cubic but tetragonal. As seen in Figs. 4(b) and 4(c), the Fe(II) and Fe(III) magnetic moments in the relaxed structure increase significantly (2.53 and $1.12\mu_B$, respectively), as the lattice constant increases. These results show that the high- and low-spin states of interfacial Fe(II) and central Fe(III) ions compete with each other through the change in strain. This increase in the Fe magnetic moments also increases the induced magnetic moments of nearest oxygen ions from 0.05 to $0.21\mu_B$. The total magnetic moments are 15.6 , 2.2 , and $2.8\mu_B$ for the superlattices with the lattice constant of bulk Fe₃O₄, bulk BaTiO₃, and average, respectively. This large difference in total magnetic moments between bulk Fe₃O₄ and other lattice constants is mainly due to the dramatic change in the magnetic moments of atom type Fe(II) as shown in Fig. 4(b).³¹ Indeed, recently magnetization jumps, which are induced by the strain due to the structural phase transition of BaTiO₃, were reported in Fe₃O₄ thin film grown on BaTiO₃ single crystal.¹⁴ Moreover, this large variation in total magnetic moments can be compared with the experimental results of Fe₃O₄/MgO, where the total magnetic moment is reduced to half the value by the strain.⁹ These changes of magnetic moments by strain are also related to the change in the spin polarization of carriers. Spin polarizations of 11, 38, and 23% are obtained¹⁷ for the superlattices with the lattice constants of Fe₃O₄, BaTiO₃, and average, respectively. Based on these results, we can simply understand the previous experiments for bias-dependent magnetoresistance.² By applying an external electric field, it is possible to change the strain of BaTiO₃,³² and then the resulting strain changes the spin polarization of Fe₃O₄, which has an influence on the amount of magnetoresistance.

C. Effect of oxygen vacancies

To see the possibility of restoring the half metallicity, oxygen vacancies are considered in the superlattice which may reduce charge imbalance at the interface. Now, for the oxygen vacancy in bulk Fe₃O₄, it was reported that the oxygen vacancies and their complexes with iron defects can be formed in bulk Fe₃O₄ when it is equilibrated with the low oxygen partial pressure at high temperature.³³ To see the possibility of oxygen vacancies, we obtained the calculated formation energy of 4.79 eV for the oxygen vacancy in the bulk Fe₃O₄ under extreme oxygen poor conditions, where the formation energy of the oxygen vacancy ($E^f[O_v]$) is defined as

$$E^f[O_v] = E_{\text{tot}}[O_v] - E_{\text{tot}}[\text{Fe}_3\text{O}_4] + 1/2E_{\text{tot}}[\text{O}_2] + 1/4\Delta H_f[\text{Fe}_3\text{O}_4], \quad (1)$$

where $E_{\text{tot}}[O_v]$ is the total energy derived from the supercell calculation with one oxygen vacancy and $E_{\text{tot}}[\text{Fe}_3\text{O}_4]$ is the

total energy for the bulk Fe_3O_4 with the same supercell size. $E_{\text{tot}}[\text{O}_2]$ is the energy of oxygen in an O_2 molecule, and $\Delta H_f[\text{Fe}_3\text{O}_4]$ is the enthalpy of formation (negative for a stable compound). Therefore, it is anticipated that it is difficult in bulk to form oxygen vacancies, as a point defect. However, recently, oxygen vacancies were also found near the film Fe_3O_4 [001] surfaces on a MgO [001] substrate by scanning tunneling microscopy (STM),^{34,35} in which the relation between oxygen-vacancy-induced surface reconstruction and the relaxation of the charge in the polar Fe_3O_4 [001] surface is discussed. By a similar compensation mechanism, our charge imbalanced system at the interface is expected to be stabilized by oxygen vacancies, as in the experiments. Therefore, the oxygen vacancies can be one of the candidates among the native defects for restoring the half metallicity near the interface of our $\text{Fe}_3\text{O}_4/\text{BaTiO}_3$ system.

Hence, we have designed a model which has two oxygen vacancies at the center plane of magnetite in the superlattice structure. The calculations with the atomic position relaxation for this model show that the effect of oxygen vacancies is simply to shift E_F to a higher energy level, and thus to recover the almost half-metallic ground state at the interface. In this strategy, it is important to keep oxygen vacancies at the central layers of magnetite since this rigid-band picture can be easily destroyed by oxygen vacancies near the interface layer. Note that the mainly interfacial Fe ions contribute to the DOS at E_F . In addition, we have found that oxygen vacancies at the central layer have a 0.25 eV lower formation energy than those at the interface layers. These oxygen vacancies in the central layer induce the large structural rearrangement in which the tetrahedral Fe ions move into interfacial Fe_2O_4 layers by as much as 1.13, 0.18, and 0.91 Å for the x , y , and z directions, respectively. By this large rearrangement, the constituent of the interfacial layer changes from Fe_2O_4 to Fe_3O_4 , which reflects the compensation of the excess charge state of the interfacial Fe_2O_4 layer induced by the oxygen vacancies. In contrast, in bulk Fe_3O_4 , the oxygen vacancy does not induce such a large rearrangement, in which the relaxed tetrahedral Fe ions are located near their bulk position. Therefore, this peculiar large structural rearrangement near the interface can be understood by the energy gain obtained from reducing charge imbalance at the interface. Moreover, the half metallicity of the central layer as a bulklike region is also conserved by forming the neutral Fe_2O_2 layer due to two oxygen vacancies, different from the bulk Fe_3O_4 where oxygen vacancies destroy half metallicity.

As for the effects of these oxygen vacancies, an enhanced spin polarization of 63% is obtained, which is much larger than the 11% spin polarization for the superlattice with no oxygen vacancy. The magnetic moment of the tetrahedral Fe(I) ion increases by as much as $0.2\mu_B$; in contrast, the octahedral Fe ions decrease their magnetic moments by as much as $0.3\text{--}0.5\mu_B$. On the contrary, in the bulk Fe_3O_4 with oxygen vacancies, the tetrahedral Fe ions near the oxygen vacancy show a decreased magnetic moment by as much as $0.2\mu_B$, which leads to the loss of half metallicity in bulk Fe_3O_4 . The changes of magnetic moments near the interface of the $\text{Fe}_3\text{O}_4/\text{BaTiO}_3$ superlattice systems originate from the shift of E_F to a higher energy level due to the oxygen vacancy, which increases the electron occupancy. The increase

in the spin polarization is consistent with this magnetic-moment behavior in the tetrahedral and octahedral Fe ions; the additional electrons mainly occupy the spin-down DOS for all Fe ions since the tetrahedral Fe ions have partially occupied spin-down (majority) and fully empty spin-up (minority) states, while the octahedral Fe ions have increasing spin-down DOS (minority) and decreasing spin-up DOS (majority) at E_F . Moreover, in our calculated results, the $3d$ states of interfacial Ti are not affected by the oxygen vacancies in the Fe_3O_4 part so it still has empty $3d$ occupancy as in bulk BaTiO_3 and in the superlattice without oxygen vacancy. This means that without destroying the insulating behavior of central layers of BaTiO_3 , the spin polarization of the carriers can be controlled by the oxygen partial pressure during the growth of Fe_3O_4 as a part of the superlattice.

When a metal contacts a ferroelectric material, the effect of screening must be considered at the interface.²⁸ However, as mentioned above, Ti ions in BaTiO_3 have empty $3d$ occupancy, and thus there is no long-range hybridization between the Fe_3O_4 and BaTiO_3 systems. This possibly indicates that Fe_3O_4 has no significant effect on the polarization instability of BaTiO_3 , and so the BaTiO_3 and Fe_3O_4 can interact with each other mainly by the strain effect. The fact that the displacements of the BaTiO_3 in the superlattice do not affect significantly the relaxed results of the Fe_3O_4 layers, which was mentioned in Sec. III B above, also supports these ideas. In this study, only the superlattices with inversion symmetry are considered so it is not appropriate to discuss the depolarizing electric field effect inside ferroelectric BaTiO_3 , which possibly affects the critical thickness for ferroelectricity. For obtaining the critical thickness of BaTiO_3 showing ferroelectricity and analyzing the relationship between the metallic interface and the ferroelectric properties, further studies in the thicker cases are needed.

IV. CONCLUSIONS

We have investigated the physical properties at the interface of a short-period multiferroic superlattice $\text{Fe}_3\text{O}_4/\text{BaTiO}_3$. A metallic ground state is obtained, which is different from the half-metallic ground state of bulk Fe_3O_4 . The loss of this half metallicity can be understood by the charge imbalance between the charged $(\text{Fe}_2\text{O}_4)^{3-}$ and the neutral $(\text{TiO}_2)^0$ layers. This metallic ground state at the interface is not expected to affect significantly the ferroelectric property of the BaTiO_3 part in the superlattice because the position of the conduction-band minimum ($3d$ states) of Ti ions is higher than the E_F of magnetite, which results in empty $3d$ states inducing the ferroelectric polarization. The displacement of ions by atomic position relaxation and the strain effect on the magnetic property are important for the application of multiferroic devices since they have a large influence on the magnetic moment of Fe ions and the spin polarization of carriers in the superlattice $\text{Fe}_3\text{O}_4/\text{BaTiO}_3$. For the recovery of half metallicity in the superlattice, the control of oxygen vacancies can be considered.

ACKNOWLEDGMENTS

This work was supported by the NSF through its MRSEC

program at the Northwestern Materials Research Center and by its NPACI supercomputing program. We are grateful to

Bruce Wessels for suggesting this problem and for discussions.

-
- ¹W. Eerenstein, N. D. Mathur, and J. F. Scott, *Nature (London)* **442**, 759 (2006).
- ²M. Ziese, A. Bollero, I. Panagiotopoulos, and N. Moutis, *Appl. Phys. Lett.* **88**, 212502 (2006).
- ³D. J. Huang, C. F. Chang, H.-T. Jeng, G. Y. Guo, H.-J. Lin, W. B. Wu, H. C. Ku, A. Fujimori, Y. Takahashi, and C. T. Chen, *Phys. Rev. Lett.* **93**, 077204 (2004).
- ⁴A. R. West, *Basic Solid State Chemistry*, 2nd ed. (Wiley, New York, 1999).
- ⁵E. Wimmer, H. Krakauer, M. Weinert, and A. J. Freeman, *Phys. Rev. B* **24**, 864 (1981).
- ⁶H. J. F. Jansen and A. J. Freeman, *Phys. Rev. B* **30**, 561 (1984).
- ⁷S. Picozzi, A. Continenza, and A. J. Freeman, *J. Appl. Phys.* **94**, 4723 (2003).
- ⁸I. Galanakis, *J. Phys.: Condens. Matter* **16**, 8007 (2004).
- ⁹Y. X. Chen, C. Chen, W. L. Zhou, Z. J. Wang, J. Tang, D. X. Wang, and J. M. Daughton, *J. Appl. Phys.* **95**, 7282 (2004).
- ¹⁰S. D. Berry, D. M. Lind, G. Chern, and H. Mathias, *J. Magn. Mater.* **123**, 126 (1993).
- ¹¹D. M. Lind, S. D. Berry, G. Chern, H. Mathias, and L. R. Testardi, *J. Appl. Phys.* **70**, 6218 (1991).
- ¹²M. Sohma, K. Kawaguchi, and T. Manago, *J. Appl. Phys.* **89**, 2843 (2001).
- ¹³G. E. Sterbinsky, J. Cheng, P. T. Chiu, B. W. Wessels, and D. J. Keavney, *J. Vac. Sci. Technol. B* **25**, 1389 (2007).
- ¹⁴H. F. Tian, T. L. Qu, L. B. Luo, J. J. Yang, S. M. Guo, H. Y. Zhang, Y. G. Zhao, and J. Q. Li, *Appl. Phys. Lett.* **92**, 063507 (2008).
- ¹⁵H.-T. Jeng and G. Y. Guo, *Phys. Rev. B* **65**, 094429 (2002).
- ¹⁶M. Friák, A. Schindlmayr, and M. Scheffler, *New J. Phys.* **9**, 5 (2007).
- ¹⁷For the calculation of spin-polarization for carriers, we used the absolute value of $[\text{DOS}(\text{up-spin})-\text{DOS}(\text{down-spin})]/[\text{DOS}(\text{up-spin})+\text{DOS}(\text{down-spin})]$ at E_F .
- ¹⁸L. Hedin and B. Lundqvist, *J. Phys. C* **4**, 2064 (1971).
- ¹⁹We compared the results using the superlattice with a half unit cell of Fe_3O_4 to the one unit cell, and obtained the same results of a ferrimagnetic metallic ground state and the same magnetic moments in both cases.
- ²⁰One and a half unit cells of BaTiO_3 used in the superlattice are too thin to see the ferroelectric displacement of Ti ions, when it is in contact with the metal (Refs. 26 and 28). It is, however, enough to see the effects of charge imbalance, strain, and oxygen vacancies because they are independent of the thickness of the BaTiO_3 slab in the superlattice.
- ²¹When the interface configurations are considered in the [001] direction, the $\text{Fe}_2\text{O}_4/\text{TiO}_2$ interface shows a much better match between the transition-metal cations (Fe and Ti ions) and the oxygen anions than does the $\text{Fe}_2\text{O}_4/\text{BaO}$ interface.
- ²²O. Jepsen and O. K. Anderson, *Solid State Commun.* **9**, 1763 (1971).
- ²³P. E. Blöchl, O. Jepsen, and O. K. Andersen, *Phys. Rev. B* **49**, 16223 (1994).
- ²⁴A. Yanase and K. Siratori, *J. Phys. Soc. Jpn.* **53**, 312 (1984).
- ²⁵N. A. Hill, *J. Phys. Chem. B* **104**, 6694 (2000).
- ²⁶C.-G. Duan, S. S. Jaswal, and E. Y. Tsybal, *Phys. Rev. Lett.* **97**, 047201 (2006).
- ²⁷P. Mavropoulos, M. Ležaić, and S. Blügel, *Phys. Rev. B* **72**, 174428 (2005).
- ²⁸J. Junquera and P. Ghosez, *Nature (London)* **422**, 506 (2003).
- ²⁹L. Kim, J. Kim, U. V. Waghmare, D. Jung, and J. Lee, *Phys. Rev. B* **72**, 214121 (2005).
- ³⁰O. Diéguez, K. M. Rabe, and D. Vanderbilt, *Phys. Rev. B* **72**, 144101 (2005).
- ³¹In the supercell used in this work, the atom types Fe(I), Fe(II), Fe(III), and Fe(IV) have 2, 4, 1, and 1 Fe atoms, respectively.
- ³²A. García and D. Vanderbilt, *Appl. Phys. Lett.* **72**, 2981 (1998).
- ³³F. Millot and Y. Niu, *J. Phys. Chem. Solids* **58**, 63 (1997).
- ³⁴B. Stanka, W. Hebenstreit, U. Diebold, and S. A. Chambers, *Surf. Sci.* **448**, 49 (2000).
- ³⁵A. Subagy and K. Sueoka, *Jpn. J. Appl. Phys., Part 1* **44**, 5447 (2005).